

## **STUDIES OF CAPILLARY POROSITY OF CLINKER PHASES DURING HYDRATION**

*A. V. Usherov-Marshak<sup>1</sup>, V. P. Sopov<sup>1</sup> and W. Kurdowski<sup>2</sup>*

<sup>1</sup>Civil Engineering Institute, Kharkov, Ukraine

<sup>2</sup>University of Mining and Metallurgy, Cracow, Poland

### **Abstract**

The capillary porosity of clinker phases, i.e.  $3\text{CaOSiO}_2$ ,  $\beta 2\text{CaOSiO}_2$ ,  $3\text{CaOAl}_2\text{O}_3$  and  $4\text{CaOAl}_2\text{O}_3\text{Fe}_2\text{O}_3$ , at the early stages of hydration has been studied by the methods of Differential Scanning Calorimetry and nitrogen adsorption (BET).

It was established that pores of 3–70 nm were formed during the hydration of  $3\text{CaOSiO}_2$  and the maximum of their distribution was found at about 10 nm. The hydration of  $2\text{CaOSiO}_2$  is much slower and the porosity is one order of magnitude lower. During the hydration of  $3\text{CaOAl}_2\text{O}_3$  the content of crystalline hexagonal hydrates prevailed and the porosity was in the range 5–90 nm with the average pore diameter of about 16 nm. This average pore diameter was much smaller for thermoporosimetry and lay at about 7 nm. The hydrated  $4\text{CaOAl}_2\text{O}_3\text{Fe}_2\text{O}_3$  sample had the porosity in the range 3–90 nm with the maximum of the pores distribution at about 4 nm. There are some differences between the porosities measured by BET and thermoporosimetry. Principally thermoporosimetry gives no information about larger capillary pores in the range 30–50 nm.

**Keywords:** BET, clinker phases, C–S–H gel, porosity, surface area, thermoporosimetry

### **Introduction**

A microstructure formation of the paste during hardening is the function of chemical reactions occurring between water and cement phases.

During this process the products of chemical reactions fill the volume previously occupied by water. These products are amorphous such as C–S–H gel and crystalline, such as calcium hydroxide, calcium aluminates and calcium sulpho-aluminates hydrates. The final microstructure of cement paste covers hydration products, unreacted cement relicts and pores, partially or fully filled with water.

Physico-chemical properties of cement paste are to a considerable degree dependent on its porosity, namely on the content of capillary pores between 2 and 100 nm [1]. These capillary pores determine durability, permeability and frost resistance of concrete [2].

\* Presented at CETTA'97, Zakopane, Poland.

There are several methods of determination of total porosity and pore-size distribution; the intrusion mercury porosimetry is the most frequently used [3].

The paper presents the results of porosity measurements of pure clinker phases during hydration.

## Experimental

Two methods were used for porosity measurements of the samples: thermoporosimetry with DSC apparatus and BET.

Thermoporosimetry is based on the utilization of Kelvin's equation and entropy of phase transformation [4, 5]; the effect of the superficial phase transformations on the entropy changes was included by Brun [6].

The BJH [7] method was used in case of BET for capillary calculation. This method is based on Cohan's [8] model.

In case of thermoporosimetry the measurements were made in the interval  $+20-60^{\circ}\text{C}$  at the cooling/heating rate of  $0.5^{\circ}\text{C min}^{-1}$ , the samples were in hermetic aluminium containers.

Before the BET measurements the samples were flushed with helium under pressure of about  $10^{-1}$  Pa. The measurements were performed with nitrogen, using the automatic ASAP 2000. For the investigation four samples of synthetic clinker phases were used:  $\text{Ca}_3[\text{SiO}_4]\text{O}$ ,  $\beta\text{Ca}_2[\text{SiO}_4]$ ,  $\text{Ca}_3[\text{Al}_2\text{O}_6]$  and  $\text{Ca}_4[\text{Al}_2\text{Fe}_2\text{O}_{10}]$ . The chemical composition of these phases is presented in Table 1.

**Table 1** Chemical composition of clinker phases

Sample	Loss of ign.	$\text{SiO}_2$	CaO	$\text{Al}_2\text{O}_3$	$\text{Fe}_2\text{O}_3$	free CaO	Total
$\text{C}_3\text{S}$	0.15	26.14	73.17	0.72	0.1	0.7	100.28
$\text{C}_2\text{S}$	0.2	34.3	64.8	trace	trace	no	99.3
$\text{C}_3\text{A}$	0.33	0.42	61.73	37.61	0.08	trace	100.17
$\text{C}_4\text{AF}$	0.13	1	45.5	20.77	32.9	0.4	100.3

The pastes were prepared from these phases with  $w/c$  ratio equal 0.5 in case of silicates and  $w/c=1$  for tricalcium aluminate and brownmillerite. The pastes were stored in the air of 100%RH and temperature  $20\pm 1^{\circ}\text{C}$  for one and three days. The phase composition of hydrated samples were examined by X-ray diffraction and SEM.

## Results

$\text{C}_3\text{S}$  underwent rapid hydration and the samples were composed of well developed fibres of C-S-H and plates of  $\text{Ca}(\text{OH})_2$  (Fig. 1).

$\beta\text{C}_2\text{S}$  reacted very slowly with water and the SEM picture presented the unhydrated grains of belite and a small quantity of amorphous C-S-H gel. Tricalcium



**Fig. 1** SEM of C<sub>3</sub>S after 1 day of hydration; plates of Ca(OH)<sub>2</sub> and fibres of C-S-H

aluminate underwent very quick hydration forming beautiful plates of 4CaOAl<sub>2</sub>O<sub>3</sub>·13H<sub>2</sub>O and small quantity of Al(OH)<sub>3</sub> gel (Fig. 2).

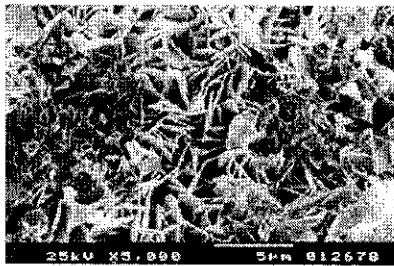


**Fig. 2** SEM of C<sub>3</sub>A after 3 days of hydration; crystals of 4CaOAl<sub>2</sub>O<sub>3</sub>·13H<sub>2</sub>O and gel Al(OH)<sub>3</sub>

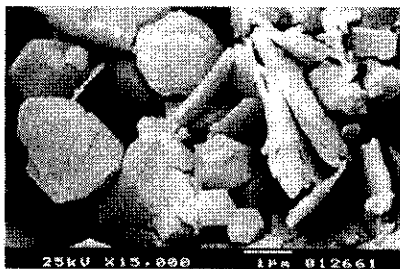


**Fig. 3** SEM of C<sub>4</sub>AF after 3 days of hydration; cubic hydrogarnet and hexagonal plates of 4CaOAl<sub>2</sub>O<sub>3</sub>·13H<sub>2</sub>O

Brownmillerite reacted quickly with water and well developed plates of 4CaO(Al<sub>2</sub>O<sub>3</sub>,Fe<sub>2</sub>O<sub>3</sub>)·13H<sub>2</sub>O appeared but, additionally, a smaller quantity of cubic hydrogarnet were formed (Fig. 3). Fe(OH)<sub>3</sub> was also present.

### *Porosity measurements*

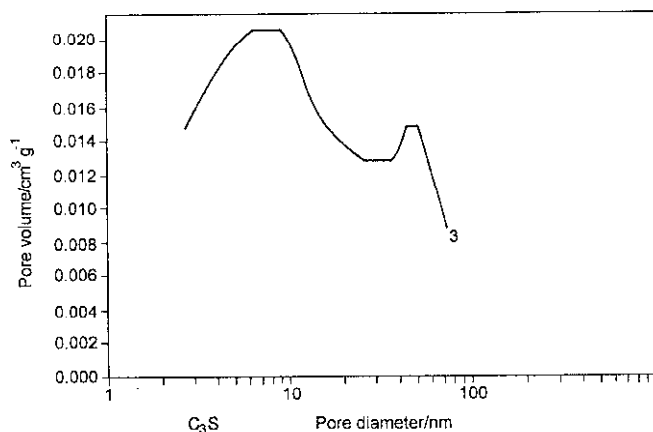
The BET measurements are collected in Table 2.

Some examples of the distribution of pore sizes are presented in Figs 4–5.

**Table 2** Results of BET measurements

Sample	Hydration/ day	Pore distribution/ nm	Average pore radius/ nm	Specific surface/ $\text{m}^2 \text{g}^{-1}$
$\text{C}_3\text{S}$	1	3–70	9.5	6.3
	3	3–70	7.4	7
$\text{C}_2\text{S}$	1	3–50	6.9	1.2
	3	3–50	6.4	1.6
$\text{C}_3\text{A}$	1	5–90	16.7	6
	3	5–90	15.5	5.5
$\text{C}_4\text{AF}$	1	2–60	7.4	5.8
	3	2–80	5.9	11.5

In case of  $\text{C}_3\text{S}$  hydration products the maximum of porosity volume is in the range of small capillary pores (Fig. 4) but the second smaller maximum is in the region of much larger pores, i.e. about 40 nm.

**Fig. 4**  $\text{C}_3\text{S}$  after 3 days of hydration;  $dv/d\log(D)$  desorption pore volume plot

Regardless the small average pore sizes the hydrated  $\text{C}_2\text{S}$  contains a large quantity of larger pores of about 50 nm in diameter. The total porosity in the range 2–500 nm, according to the BET measurements, was very small and resulted in 0.0016 and 0.002 for 1 and 3 days of hydration, respectively. The maximum porosity volume for the  $\text{C}_3\text{A}$  hydrated sample is between 30 and 40 nm of pores diameter (Fig. 5). Hydrated brownmillerite (Fig. 5) has a very sharp maximum of porosity for a pore diameter of 3 nm and a broad maximum range of pores diameter of 60–70 nm.

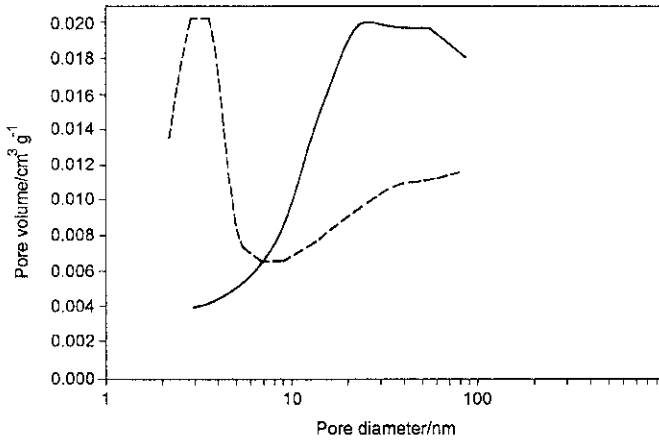


Fig. 5 C<sub>3</sub>A and C<sub>4</sub>AF (dashed line) after 3 days hydration;  $dv/d\log(D)$  desorption pore volume plot

A slightly different picture presents the thermoporosimetry for the hydrated C<sub>3</sub>S sample and the existence of two regions of pores distribution in the range 2–8 nm (Fig. 6) was found.

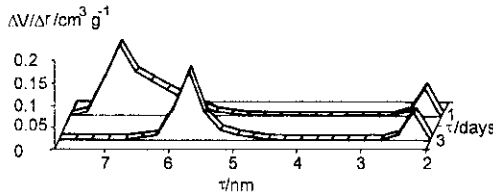


Fig. 6 Thermoporosimetry of the sample of hydrated C<sub>3</sub>S

The first maximum is in the range the pores radius of about 2 nm. During hydration from 1 to 3 days this maximum remains in the same position, but the second maximum for 6–7 nm pore radius is shifted a little after 3 days of hydration to about 6.5 nm. It should be noted that Colleparidi found the maximum at 2 nm for hydrated C<sub>3</sub>S [9].

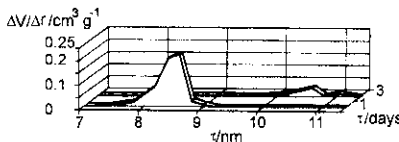


Fig. 7 Thermoporosimetry of the sample of hydrated βC<sub>2</sub>S

Figure 7 presents the results for the hydrated βC<sub>2</sub>S sample. The small degree of hydration found its expression in a larger pores diameter because as it is well known, the phase composition after hydration of dicalcium silicate is very similar to that of C<sub>3</sub>S [10].

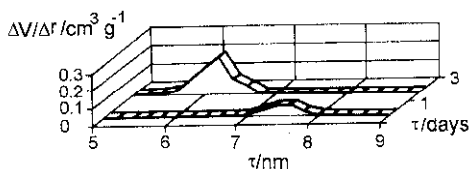


Fig. 8 Thermoporosimetry of a hydrated sample of  $C_3A$

As we observed previously, the aluminate is quickly hydrated with the formation of crystalline  $C_4AH_{13}$  but also  $AH_3$  gel. The results of thermoporosimetry showed the presence of pores only in one range between 7 and 8 nm after one day of hydration and 5 and 7 nm after 3 days (Fig. 8).

The thermoporosimetry of the sample of hydrated  $C_4AF$  also showed one range of porosity, similar to tricalcium aluminate (Fig. 9).

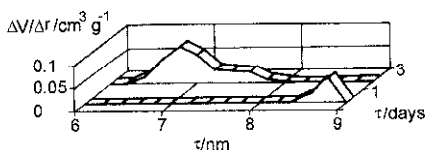


Fig. 9 Thermoporosimetry of hydrated sample of  $C_4AF$

The pores distribution in the function of porosity had a maximum one day of hydration for 8.8 nm and after three days at 6.8 nm.

The capillary porosity in the range of 2 to 100 nm showed a decrease between one and three days of hydration. According to thermoporosimetry measurements this decrease was: for  $C_3S$  from 0.22 to 0.12  $cm^3 g^{-1}$  and for BET 0.0259  $cm^3 g^{-1}$  for one day and 0.0248  $cm^3 g^{-1}$  for three days. As it can be seen from this comparison, the BET porosity is one order of magnitude smaller. However, for both methods the porosity decreases during hydration.

For the hydrated  $C_3A$  samples these values were: for thermoporosity 0.036  $cm^3 g^{-1}$  for one day of hydration and 0.099  $cm^3 g^{-1}$  for three days, for BET 0.03249 and 0.021185  $cm^3 g^{-1}$ , respectively.

The results in this case are much closer for two methods. However, according to BET, the porosity decreases between one and three days of hydration and for thermoporosity the opposite result is valid.

In case of the  $C_4AF$  samples BET gave a lower value of porosity, i.e. 0.0137  $cm^3 g^{-1}$  after one day and 0.0181 after three days. On the other hand however, the results of thermoporosity measurements were: 0.0266 and 0.0567  $cm^3 g^{-1}$  for one and three days, respectively. In this case the increase of porosity is observed for both methods.

It must be taken into account that the range of measurements is not identical with two methods and for thermoporosity it is between 2 and 100 nm while for BET it is much larger and is between 2 and 500 nm. In this connection the big

difference of porosity, i.e. much larger porosity for  $C_3S$  is not clear and needs further examination.

The BET method gave also some increase of porosity for larger capillary pores, namely for  $C_3S$  in the range of 50 nm and for  $C_3A$  a broad maximum in the range of 20–50 nm. Also for the  $C_4AF$  sample after one day of hydration this second maximum for 30–50 nm was found. There was no maximum in this area on the curves obtained in thermoporosimetry measurements. However, the average pore diameter is quite close for both methods. For example, this diameter for  $C_4AF$  after one day of hydration is: 8.8 and 7.4 nm, according to thermoporosimetry and BET, respectively. After three days of hydration: 6.8 and 5.9 nm, respectively.

## Conclusions

1. BET method gives a lot of information about the structure of hydrated clinker phases. The surface area is dependent chiefly on the velocity of hydration and on amorphous phases formation.

2. The porosity measurements by thermoporosimetry and BET can give relatively large differences, especially for samples rich in amorphous phases. In case of dominance of crystalline hydration products the differences are less pronounced.

3. The thermoporosimetry measurements give no information about the larger capillary pores in the range 30–50 nm.

4. The results of porosity studies by BET and thermoporosimetry can be useful for modelling of the structure of hardened cement paste.

## References

- 1 R. Brunauer, R. S. Mikhail and E. E. Bodar, *J. Colloid. Interface Sci.*, 24 (1967) 451.
- 2 S. Goto and M. Daimon, *Proc. 8th ICCR Rio de Janeiro*, Vol. VI, 1986, p. 405.
- 3 J. Sellevold and H. Bager, *Proc. 7th ICCR Paris*, Vol. IV, 1980, p. 394.
- 4 A. V. UsheroV-Marshak and V. P. Sopov, *J. Thermal Anal.*, 45 (1995) 497.
- 5 S. Matala, *Proc. 10th ICCR Gotenburg*, Vol. 3, 1997, p. 3v017.
- 6 M. Brun, A. Lallemand, J.-F. Quinson and C. Eurand, *Thermochim. Acta*, 21 (1917) 59.
- 7 P. Eliot, E. P. Barret, L. G. Joyner and P. P. Halenda, *J. Am. Chem. Sci.*, 73 (1951) 373.
- 8 L. H. Cohan, *J. Am. Chem. Soc.*, 60 (1944) 98.
- 9 M. Collegardi, *Proc. RILEM/IVPAC, Int. Symp. Pore Structure and Properties of Materials*, Praga, Vol. 1, 1973, p. B25.
- 10 H. F. W. Taylor, *Proc. 8th ICCR Rio de Janeiro*, Vol. 1, 1986, p. 83.